*Journal of Thermal Analysis and Calorimetry, Vol. 59 (2000) 483–495*

*Dedicated to Prof. Edith A. Turi in recognition of her leadership in education*

# QUIESENT CRYSTALLIZATION KINETICS OF NUCLEATED METALLOCENE AND ZN ISOTACTIC POLYPROPYLENES

*Manika Varma-Nair*[1] *and P. K. Agarwal*[2]

[1]Corporate Research, ER&E, Annadale, NJ
[2]Exxon Chemical Company, Baytown, Houston, TX, USA

## Abstract

Crystallization kinetics and thermodynamic properties of nucleated isotactic polypropylene (PP) are analyzed using Hoffman–Lauritzen crystallization theory to determine the mechanistic effects of the nucleators. Calorimetric data provides quantitative comparisons between nucleating efficiences of the α (Millad) and β (NJSTAR) nucleator in Metallocene (M) and Ziegler–Natta (ZN) PP. The two types of PP without nucleators showed similar crystallization behavior though the $T_m^o$ for ZN-iPP was about 10°C higher than M-iPP. Both nucleators show significant improvement in crystallization rate in both types of PP. In addition, Millad outperforms NJSTAR. The magnitude of the kinetic response is, however, different and both the nucleators appear to function better in ZN than in Metallocene PP. β nucleated PP shows predominantly the β form. The amount of the β form is thermal history dependent and changes with supercooling ($\Delta T=T_m^o-T_c$). Similar equilibrium melting temperature ($T_m^o$) in the α nucleated and control PPs indicates the lack of any thermodynamic effect of the α nucleator. All nucleated PPs show a much lower secondary nucleation rate constant, $K_g$.

**Keywords**: α-β-nucleators, crystallization kinetics, equilibrium melting temperature, Hoffman–Lauritzen analysis, Metallocene and Ziegler–Natta isotactic polypropylenes, thermodynamic properties

## Introduction

Crystallization of conventional ZN-iPP from melt in the presence of nucleators is widely reported in the literature [1]. Typically nucleating agents increase the crystallization rate [2]. Depending on the process and the desired morphology and properties, heterogenous nuclei such as solids, liquids and even gas bubbles have been used as nucleators [1]. Metal salts and the newer sorbitol based nucleators are some of the commonly used nucleators. Broadened melting range is also reported by addition of propylene copolymers and certain inorganic additives. Presence of nucleating agents such as quinacridone dyes are known to produce 100% of the lower melting (145–150°C), β-form under appropriate thermal conditions of crystallization [3]. By varying nucleator type and concentration, an optimum combination of α and β form can be obtained to achieve the maximum benefit of the two forms of PP [4]. This ap-

*1418–2874/2000/ $ 5.00*
*© 2000 Akadémiai Kiadó, Budapest*
*Akadémiai Kiadó, Budapest*
*Kluwer Academic Publishers, Dordrecht*

proach in principle can provide an increase in crystallization rate and broadened melting range of PP desired in certain PP processes and applications.

The main objective of the present work was to analyze the kinetic aspects of nucleated Metallocene PP and determine quiescent crystallization kinetics and thermodynamic properties. Though literature is abundant with such studies for ZN-iPP [e.g., 5], not much work is reported on the M-iPP [6, 7]. In this paper calorimetry is used to obtain the temperature dependent rates of crystallization and crystallization is analyzed using Hoffman–Lauritzen's secondary nucleation theory for polymer crystallization. Both α (Millad) and β (NJSTAR) nucleators are evaluated. Heat capacity measurements are used to analyze the melting behavior to determine their effects. The results of the kinetic analysis are used to judge performance of various nucleated PPs.

## Experimental

The details of the ZN and M-iPP with and without nucleators are given in Table 1, column 1. The α and β nucleators used are Millad [bis(3,4-dimethylbenzylidene sorbitol) and NJSTAR (N,N'-dicyclohexyl-2,6-naphathalene dicarboxamide) respectively. The melt flow rate MFR, of ZN-iPP and M-iPP was 2.0 and 2.8 respectively. $M_w$ and $M_n$ for ZN-iPP were 419000, 113000 and for M-iPP were 323000 and 121000. A TA instruments MDSC 2920 equipped with an autosampler and a liquid nitrogen cooling accessory was used for the measurements of heat capacities from –140 to 220°C using the conventional technique. All the measurements were carried out on as received samples cooled to –140°C and heated at 10°C $min^{-1}$ and also on samples where thermal history was destroyed by melting at 210°C for 5 min and then cooling them to –140°C before measurement. All experimental heat capacities are corrected with a sapphire standard using National Institute of Standards (NIST) $C_p$ data.

Isothermal kinetic measurements were carried out on the PE-DSC7 equipped with an intracooler. Measurements were done at various isothermal temperatures ranging from 104–146°C in 2°C intervals. In all cases the sample was first heated to 210°C to destroy the thermal history, held for 5 min and fast cooled to the isothermal temperature and held for either 20 or 30 min. Half time for crystallization was obtained as time taken for 50% crystallization. Melting traces of the isothermally crystallized samples were analyzed to obtain the thermodynamic and kinetic data.

## Results and discussion

*Phase transitions in nucleated ZN and M-iPP*

Crystallization behavior

Crystallization data on cooling at 10°C $min^{-1}$ are plotted in Fig. 1 for M-iPP. Table 1 the data for ZN-iPP. Both M-iPP and ZN-iPP crystallized at 118°C and indicate a similar crystallization behavior in these PP samples. Both α and β nucleated PPs show evidence of nucleation activity as crystallization occurred earlier in the nucle-

ated PP. Increase in nucleation density in presence of nucleators reduces the barrier to crystallization and increases the crystallization rate. 2000 ppm of α nucleator raised the crystallization temperature of ZN-iPP by 12°C while $T_c$ advanced by 8°C for M-iPP. Effect of a similar α nucleator on the crystallization of polyethylene oxide is reported in the literature [8]. It was shown that sorbitols undergo physical gelation in the polymer melt prior to crystallization and these dispersed gels promote crystallization via epitaxial crystal growth.

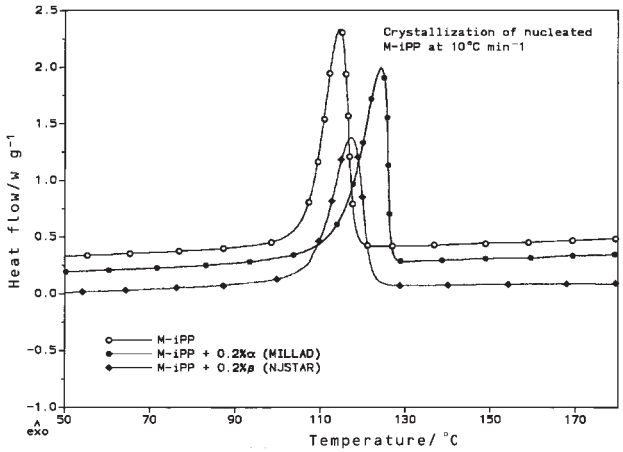


**Fig. 1** Crystallization of various nucleated Metallocene PPs

β nucleator is less effective than Millad at similar concentrations in both types of PP as it shows a smaller increase in $T_c$ than the α nucleator. In addition, the response of the β nucleator in the two types of PPs is also different. $T_c$ is increased by about 6.5°C in ZN-iPP while in M-iPP the increase was much less (3.7°C). While Millad merely promotes crystallization of the α crystals, the β nucleator in addition gives rise to a different morphological form (hexagonal) [4] that is less stable than the monoclinic α crystals.

## Melting behavior

Since thermal properties change with thermal history, the nucleated and control PP were analyzed as-received (samples obtained from extruded sheets) and melt crystallized**.** Table 1 shows the thermodynamic data for all the as-received samples and those crystallized from the melt at 10°C $min^{-1}$ are listed in parenthesis. All measurements were done at a heating rate of 10°C $min^{-1}$. Figure 2 shows the melting traces for Metallocene samples crystallized from the melt at 10°C $min^{-1}$. Melting occurs about 10°C lower in M-iPP than ZN-iPP (Table 1). The extrapolated onset of melting for the second heats (melt crystallized samples) is clearly lowered in presence of the nucleators. The peak melting does not change for α nucleated PPs indicating similar thermodynamic behavior as the PP

**Table 1** Thermodynamic properties of M-iPP and ZN-iPP with and without nucleators (α or β)

| Sample ID | Crystallization | | Glass transition | | Melting endotherm[a] | | | |
|---|---|---|---|---|---|---|---|---|
| | $T_{onset}$/ °C | $T_{peak}$/ °C | $T_g$/ °C | $\Delta C_p$/ J (K mol)$^{-1}$ | $T_{onset}$/ °C | $T_{peak}$/ °C | $\Delta H_m$/ J g$^{-1}$ | Crystallinity[b]/ % |
| ZN-iPP (cycled) | 118.0 | 112.9 | –3.2 | 7.4 | 145.9 (151.8) | 163.5 (161.9) | 86.3 (94.7) | 41.7 (45.7) |
| ZN-iPP + 0.2% α (cycled) | 129.6 | 126.6 | –3.0 | (8.0) | 150.1 (145.9) | 162.8 (164.2) | 90.0 (94.5) | 43.4 (45.6) |
| ZN-iPP + 0.2% β (cycled) | 124.4 | 121.2 | –4.3 | (5.5) | 137.2, 154.3 (144.5, small) | 143.9,164.6 (151.5, 165.5) | 42.4, 45.1 (71.5, 14.3) | 20.4, 21.8 (34.5, 6.9) |
| M-iPP (cycled) | 117.7 | 114.8 | –1.6 | (6.0) | 142.2 (146.5) | 154.8 (154.2) | 85.3 (92.4) | 41.2 (44.6) |
| M-iPP + 0.2% α nucl. | 125.6 | 123.0 | 0.4 | (5.0) | 143.3 (142.5) | 154.4 (154.2) | 90.5 (97.6) | 43.7 (47.1) |
| M-iPP + 0.2% β nucl., (cycled) | 121.4 | 117.8 | 0.8 | (8.0) | 127.9, 144.4 (137.8, small) | 139.0, 155.3 (145.1, 154.8) | 48.3, 39.9 (69.4, 14.1) | 23.3, 19.3 (33.5, 6.8) |

[a] Melting corresponds to the change of stable α form to isotropic melt. [b] All crystallinity data are obtained using 8.7 kJ mol$^{-1}$ as equilibrium heat of fusion for 100% crystalline PP. Beta nucleated ZN-iPP and M-iPP show double melting transition, first one corresponds to the melting of β crystals and the second is due to α crystal melting Crystallization data were obtained on cooling fresh samples from the melt
Lower $\Delta C_p$ at the glass transition temperature is due to the presence of 'rigid-amorphous' fraction in both types of PPs [9].

without nucleators. For the melt crystallized, α nucleated M-iPP, a small shoulder at about 145°C is clearly evident in addition to the main melting peak at about 155°C. This broad endotherm appears to be a unique feature of the nucleated M-iPP and is not clearly evident in the M-iPP without nucleators. This corresponds to the low melting α crystals that upon annealing melt at higher temperature [9]. This peak should, therefore, not be confused with the β form obtained in β nucleated M-iPP.

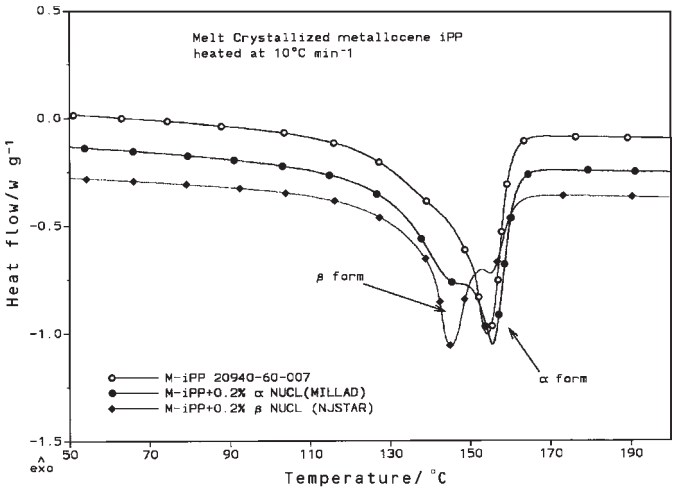


**Fig. 2** Melting of various nucleated Metallocene PPs crystallized from the melt at 10°C $min^{-1}$

β nucleated PP in both ZN and M-iPP results in a lower melting β form that is present along with the higher melting α form (Table 1). Ratio of these two forms is thermal history dependent. Melt crystallized β nucleated ZN-iPP shows predominantly (~34%) β form that melts lower at 151°C. The as-received ZN-iPP samples contained about 20% β and 22% α form. The β form is obtained using the equilibrium heat of fusion of 8.7 kJ $mol^{-1}$ of the α form. Varga [2] reports a much lower value for equilibrium heat of fusion of 4.75 kJ $mol^{-1}$ for the β form. Using this value the β form for the melt crystallized sample is estimated to be 63.2%. This together with the α form accounts for 77.5% crystallinity. This appears to be a rather high value for crystallinity for this sample and suggests that the equilibrium heat of fusion for the β form is higher than that reported by Varga [2].

For the melt crystallized β nucleated M-iPP, β form was also about 34%. As-received M-iPP had 23% β form and 19% α form. Figure 3 shows the effect of thermal history. All the relevant transition data are listed in Table 1. Thus the metastable β form transforms into the more stable α form and both types of PP have roughly the same amount of β crystals relative to the α form. To identify the breadth of melting, liquid heat capacities were extrapolated to lower temperature. β nucleated PPs show comparable breadth (about 60°C) for the melting transition and this is

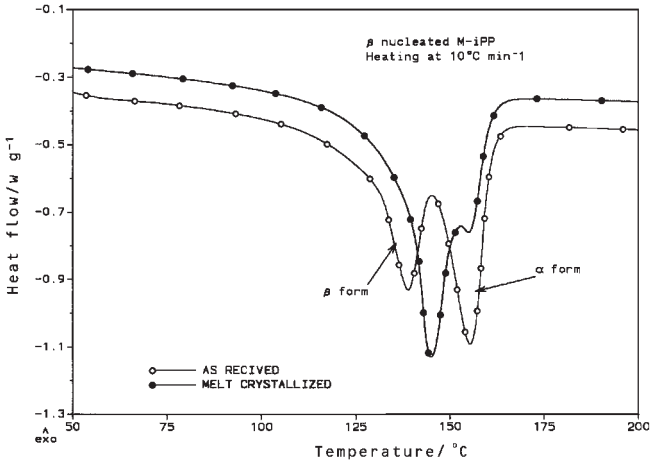


**Fig. 3** Melting of as-received and melt crystallized β nucleated M-iPPs

slightly larger (5–6°C) than that for PP without nucleators. Similar effect in increase in onset of melting is also seen in the extrapolated onset for melting listed in Table1.

*Isothermal crystallization kinetics*

The dynamics of crystal formation was determined from the melting behavior of crystals formed at various isothermal temperatures for nucleated and unnucleated PP. Melting behavior of isothermally crystallized control ZN-iPP and M-iPP are plotted in Figs 4a and 4b. Effects of supercooling ($T_m$–$T_c$) on the crystallization of PP are widely reported in the literature [2]. A summary of the observations for these control samples is provided to compare the effects of nucleators. At higher supercoolings (below 120°C in Fig. 4b), small amount of metastable β crystals (melt at about 155°C) are obtained in ZN-iPP, in addition to the higher melting α monoclinic form. Melting temperature of the α crystals increased with increase in $T_c$. A noteworthy difference between presently analyzed ZN and M-iPP is the presence a low temperature endotherm at about 145°C in M-iPP obtained at higher $T_c$. With an increase in supercooling this endotherm shifts to higher temperature and finally merges with the melting that corresponds to the α crystals. As mentioned above, this low temperature endotherm in M-iPP is due to the presence of poorly formed, small α crystals that upon annealing melt at a higher temperature [9].

Melting at various supercoolings for α nucleated PP corresponds to only α crystals. At crystallization temperatures as low as 106°C, there was no evidence of the presence of β crystals that were observed in the control ZN samples (Fig. 4b). The nucleating effect of Millad is clear in the increase in the melting of α crystals. Supercooling effects the formation of the low melting endotherm. At higher supercoolings the smaller α crystals progressively anneal to melt at higher temperatures and the low temperature endotherm almost disappears. At lower supercoolings ($T_c$>130°C), an increasing amount of both the lower and the higher melting α crystals are obtained and

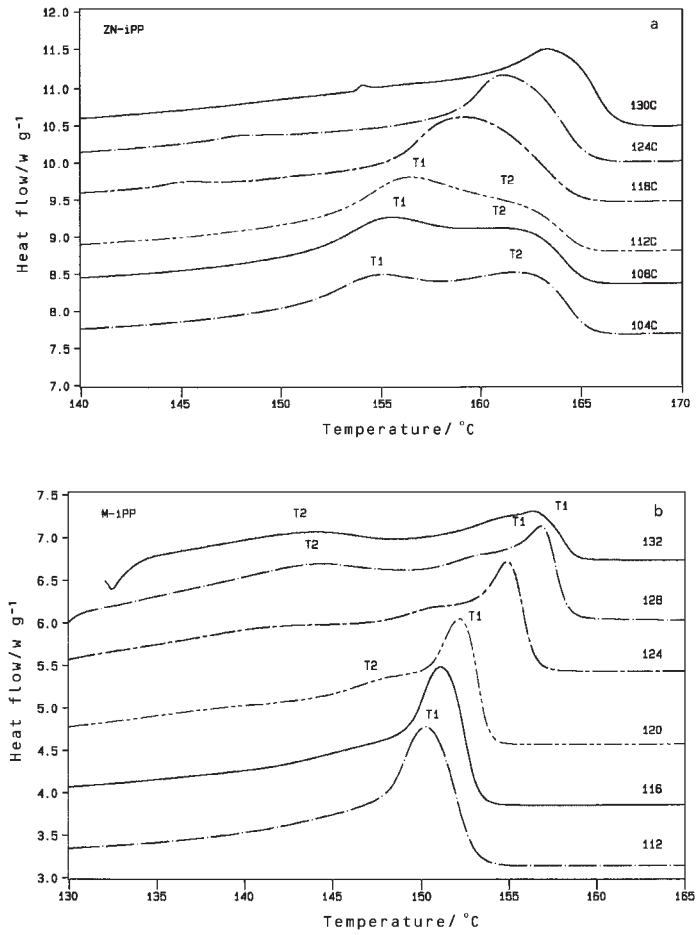


**Fig. 4** Melting of ZN-iPP (a) and M-iPP (b) isothermally crystallized for 30 min at various temperatures

a bimodal melting is observed. The effect of supercooling on the fate of low temperature endotherm is reverse of what was observed for the β crystals (Fig. 5).

Figure 5a shows the dynamics of formation of the β crystals in ZN-iPP nucleated with β nucleator. As expected, increase in supercooling results in increasing amount of β form in both PPs and at very high supercoolings (<106°C) almost all of the β crystals are obtained. Varga 1992 [10] and Fillon 1993 [11] have shown that α form can arise on partial melting of the β spherulites. β form contains only unidirectional helices contrary to the α form which is packed with alternating right and left handed helical chains. Hence a β to α transition requires rewinding of chains and this is possible only through partial melting of β form. Thus at all the isothermal temperatures measured, we always see a small α peak in PP which may have formed through the process described above. An-

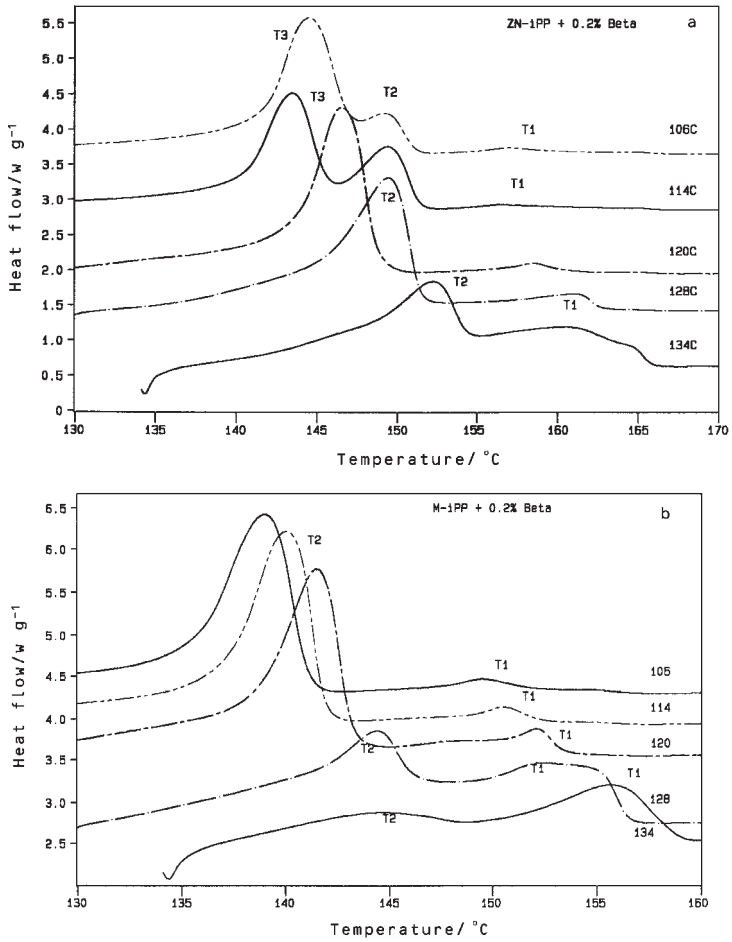


**Fig. 5** Melting of ZN-iPP (a) and Mi-PP (b) nucleated with 0.2% β nucleator and isothermally crystallized for 30 min at various $T_c$

other striking difference between the β nucleated ZN and M-iPP (Fig. 5b) is the presence of an additional endothermic peak at 155°C in ZN-iPP when $T_c$ was less than 116°C. This probably arises from melting and reorganization of the existing β form that leads to more stable crystals which melt at a higher temperature.

*Equilibrium melting temperature of nucleated PPs*

Prior to evaluating the kinetic effect of the nucleators, it is necessary to establish the equilibrium thermodynamic properties of nucleated PPs. The equilibrium melting temperature ($T_m^o$) is obtained by extrapolating the peak melting temperature ($T_m$) with respect to

the isothermal crystallization temperature ($T_c$) using Hoffman–Weeks analysis [12] where:

$$T_m=[T_m^o(1-1/\beta)+T_c/\beta] \quad (1)$$

where β represents the ratio of the final lamellae thickness to the initial critical thickness. The value of $T_m^o$ obtained in the present analysis was 185°C for ZN-iPP and about 180°C for M-iPP. The experimental melting temperatures for nucleated PPs are plotted *vs*. the crystallization temperature in Figs 6 and 7. In PP, higher $T_m^o$ can be obtained due to the lamellar thickening process that occurs at various crystallization temperatures. Crystals produced at low supercoolings thicken more than those that are produced at higher supercooling [13]. In the present experiments, PP was crystallized for 30 min. Even during this time the effect of lamella thickening is visible as the end of melting shows higher values at lower $T_c$. Only the peak temperature extrapolation is used to determine the value of $T_m^o$. The break in slope of the data at about 132–134°C is associated with the regime II–regime I transition to be discussed later [5].

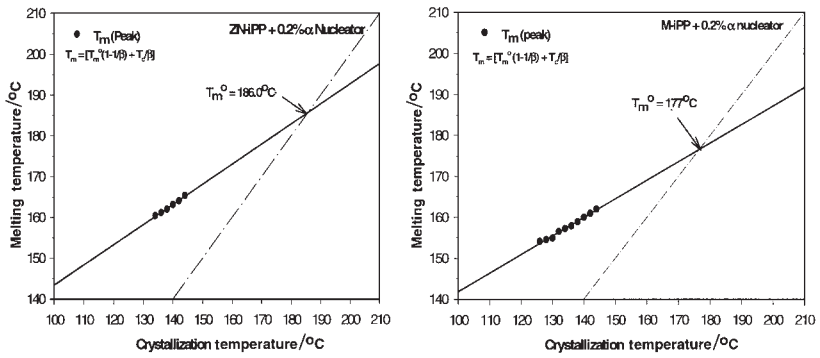


**Fig. 6** Analysis of equilibrium melting temperature of 0.2% α nucleated ZN-iPP and M-iPP

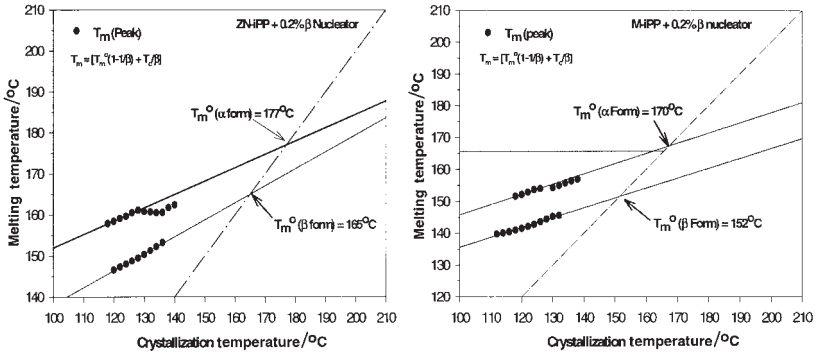


**Fig. 7** Analysis of equilibrium melting temperature of 0.2% β nucleated ZN-iPP and M-iPP

α nucleator does not change the thermodynamic state of the nucleated α crystals in either of the two polymers (Fig. 6). The nucleator merely effects kinetics which will be discussed in the next section. The β nucleated PP shows both types of crystals and therefore two $T_m^o$ are obtained. Since β crystals in ZN tend to reorganize to higher melting more stable crystals, the value of $T_m^o$ for β form is higher (165 compared to 152°C in M-iPP in Fig. 7). A $T_m^o$ value of 174.5°C for β crystalline form is reported in the literature [4] and is based on small-angle and wide-angle X-ray diffraction techniques.

*Crystallization rate from half time analysis*

Rate of crystallization is obtained using the time ($t_{1/2}$) taken for 50% crystallization to occur. The results of the analysis are plotted in Fig. 8. Both PPs without nucleators show similar crystallization kinetics. Crystallization rate of supported *vs*. unsupported M-iPP is effected by the level of defects in the polymer. Possibly these catalysts change the sequence distribution of the crystallizable PP sequences. Similar crystallization rate in the two PPs could thus arise due to the presence of long enough crystallizable sequences in the Metallocene PP. Sequence distribution in PP can be determined using calorimetry [14]. In this experiment the sample is crystallized in steps of 10°C and at each step it is annealed in the calorimeter for 4 h. The sequence distribution of the crystallizable PP sequences in the two polymers is then qualitatively assessed from the melting traces of the thermally segregated polymer. Figure 9 shows the plot for ZN and M-iPP. Each peak represents a population of PP sequences. Metallocene PP clearly has a small amount of PP sequences that are long enough to melt at a higher temperature (melting peak is about 165°C). (Note: This melting peak is only detected when the sample is cooled using the step isothermal crystallization method thus indicating that these initially formed crystals grow upon annealing). It is thus possible that these longer sequences enable Metallocene PP to crystallize at almost the same temperature as the ZN-iPP.

As seen in the increase in crystallization temperatures, nucleators increase crystallization rate of PP. Using the change in the crystallization half time as the magnitude of the

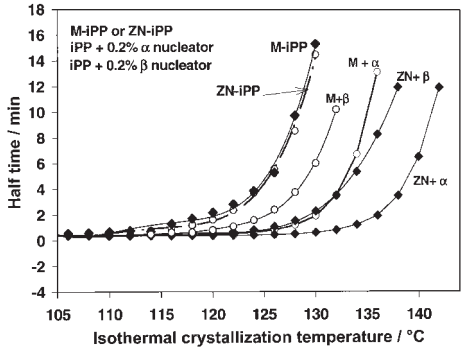


**Fig. 8** Effect of nucleators on rate of crystallization obtained from $t_{1/2}$

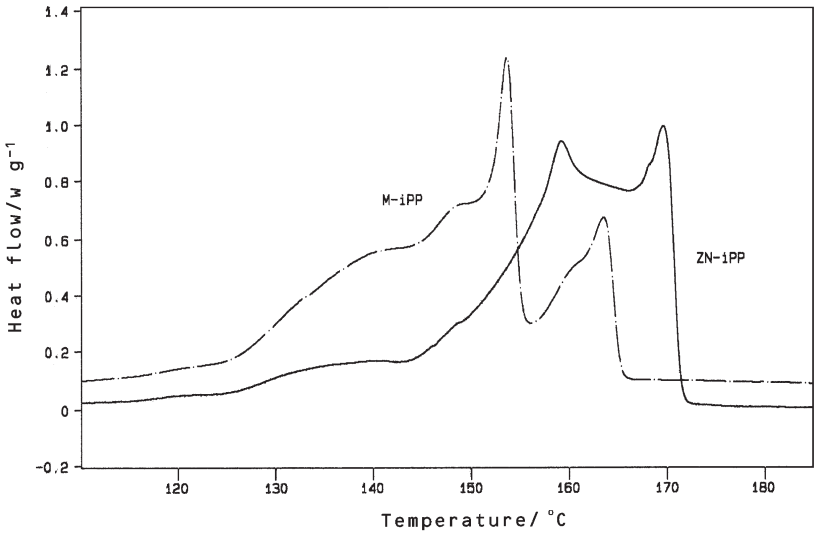


**Fig. 9** Thermal segregation in Metallocene and ZN-iPP

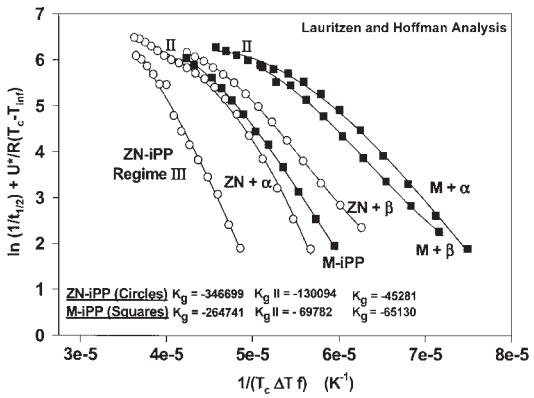


**Fig. 10** Temperature dependence of linear growth rate

increase in rate of crystallization can be determined. Clearly the α nucleator appears to be better than β in both PPs. In addition, both nucleators are more effective in ZN-iPP than in M-iPP. Since both PPs without nucleators had similar kinetics, the different response to the nucleators indicates that mechanistically the nucleators interact differently with the two polymers at the nucleation stage.

*Crystal growth rates and regime analysis*

The equlibrium melting temperature ($T_m^o$) and the crystallization half time ($t_{1/2}$) can further be used to extract the nucleation parameters to understand the mechanism of crystal-

lization in nucleated PP. We have used the well established Lauritzen–Hoffman theory for secondary nucleation in polymers [15, 16]. The theory analyzes the crystal growth data according to the competition between the rate of deposition of secondary nuclei and the rate of lateral surface spreading. The linear growth rate $G$ of polymeric spherulites or axialites is given by the equation:

$$G=G_o \exp [-U^*/R(T_c-T_\infty)] \exp [-K_g/(T_c \Delta Tf)] \quad (2)$$

$U^*$ is the activation energy for polymer diffusion across the phase boundary. We have used a value of 6276 J mol$^{-1}$ given in the literature [17] for our calculations. The equilibrium melting temperature described above were used in the calculations. A glass transition value of 0°C was used. $T_\infty$ is the temperature below which polymer diffusion ceases ($T_\infty=T_g-30$ K). The growth rate '$G$' was approximated by the half time for crystallization plotted in Fig. 8. The second exponential in Eq. (2), represents the Gibbs free energy contribution for growth of a critical size surface nucleus. It is dependent on the degree of supercooling ($\Delta T$). The factor '$f$' is the correction factor for variations in heat of fusion and is given by $2T_c/(T_c+T_m^o)$. $K_g$ is the nucleation rate constant and is evaluated by rearranging Eq. (1) as follows:

$$\ln (t_{1/2})+[U^*/R(T_c-T_\infty)]=\ln G_o-K_g[1/(T_c \Delta Tf)] \quad (3)$$

**Table 2** Kinetic data of crystal growth for nucleated PPs

| Sample | $T_m^o$/ K | $T_c$ range/ °C | $10^{-5}$ Kg/ K$^2$ | (Kg/$T_m^o$) $\propto\sigma\sigma_e$/ erg$^2$ cm$^{-4}$ |
|---|---|---|---|---|
| ZN-iPP | 184.5 | 130–104 | 3.5 | 757 |
| ZN-iPP+0.2% α | 185.0 | 130–104 | 1.3 | 284 |
| | | 130–140 | 3.5 | 770 |
| ZN-iPP+0.2% β | 165.0 | 130–110 | 0.45 | 103 |
| M-iPP | 180.0 | 130–114 | 2.7 | 591 |
| M-iPP+0.2% α | 177.0 | 120–108 | 0.7 | 160 |
| | | 136–122 | 2.0 | 440 |
| M-iPP+0.2% β | 152.0 | 132–108 | 0.65 | 145 |

σ is the lateral surface free energy, $\sigma_e$ is the fold surface energy

Using Eq. (3), the kinetics data are plotted in Fig. 10. Slope of the plots gives a measure of $K_g$ the nucleation rate constant. It is a measure of the free enthalpy of formation of a secondary nucleus with a critical size depending on the mechanism of growth. The relevant kinetic data are given in Table 2. $K_g$ for unnucleated ZN-iPP was 346699 K$^2$. An analysis of the growth data indicates that in the temperature range of measurements reported in this paper, PP without nucleants, crystallization occurs in regime III [5, 16]. This assignment is made based on the supercooling range of 30–70°C investigated. This regime corresponds to the case where secondary nucleation '$i$' >> than lateral growth '$g$'. $K_g$, was, lower for M-iPP than ZN-iPP while these two polymers showed similar $t_{1/2}$. This lower $K_g$ is related to the differences in $\sigma_e$, chain folding energy ($\sigma_e \propto K_g/T_m^o$) between the two polymers as described in the earlier report [9]. Lower fold surface energy reflects

more chain folding irregularities in Metallocene PP. The two polymers studied had a melt flow ratio (MFR), of 2.8 and 2.0 for M-iPP and ZN-iPP respectively, and thus the similarities in kinetics are noteworthy.

In presence of nucleators, supercooling is reduced as crystallization occurs at a higher temperature but the equilibrium melting does not change. Figure 10 shows two distinct slopes for the nucleated PPs that do not conform to a regime change commonly observed for PP at higher supercoolings [5, 16]. High molecular mass PP is well known to crystallize in regime II and III [5, 16] and regime I has only been reported for low molecular mass PP [5]. In the present analysis the effect of nucleators causes a slope change in the wrong direction. Nucleation changes with temperature but in the plots with the nucleators (Fig. 10) the curve at higher supercoolings is unusual. This does not reflect radial growth rate that is assumed in Eq. (3). In the derivation of Eq. (3), the effect of nucleation is not separated from crystal growth. Hence the use of this equation to interpret the effect of nucleators may not be a valid choice. In that case the quantitative estimates need to be treated with caution.

* * *

The authors wish to thank Jim Balogh for conducting the calorimetry and kinetic experiments. Prof. B. Wunderlich and Prof. Paul Phillips from the University of Tennessee are acknowledged for their valuable suggestions and comments.

## References

1 A. Galeski in 'Polypropylene Structure, Blends and Composites', Vol. 1, Ed., J. Karger-Kocsis, Chapman and Hall, New York 1995.
2 J. J. Varga, J. Thermal Anal., 31 (1986) 165, ibid., 35 (1989) 189.
3 A. J. Lovinger, J. O. Chu and C. C. Gryte, J. Polym. Sci., Polym. Phys. Ed., 15 (1977) 641.
4 P. J. Phillips and K. Mezghani, 'Polypropylene, polymorphism', in Polymeric Encyclopedia, Ed., J. C. Salmone, Vol. 9, 1996, p. 6637.
5 S. Z. D. Cheng, J. J. Janimak and A. Zhang, Macromolecules, 23 (1990) 298.
6 J. R. Isasi, L. Mandelkern and R. G. Alamo, ACS Polymer Preprints, Vol. 37, (2), August 1996, p. 239.
7 E. B. Bond and J. E. Spruiell, ANTEC 97 (1997) 1750.
8 A. Thiery, C. Straupe, B. Lotz and J. C. Whittmann, Polymer Comm., 31 (1990) 299.
9 M. Varma-Nair and P. K. Agarwal, ACS Proceedings, Polymeric Materials Science and Eng., Vol. 81, 1999, p. 310.
10 J. Varga, J. Material Sci., 27 (1992) 2557.
11 B. Fillon, B. Lotz and A. J. Thierry, J. Polym. Sci., Polym. Phys. Ed., 31 (1993) 1407.
12 J. D. Hoffman and J. J. Weeks, J. Res. Natl. Bur. Std., USA, Sect A, 66A (1962) 13.
13 K. Mezghani, R. A. Campbell and P. J. Phillips, Macromolecules, 27 (1994) 997.
14 M. Y. Keating and E. F. McCord, Thermochim. Acta, 243 (1994) 129.
15 J. I. Lauritzen and J. D. Hoffman, J. Appl. Phys., 44 (1973) 4340.
16 P. Phillips, J. Polym. Prep. (Am. Chem. Soc. Div. Polym. Chem.), 20 (1979) 438.
17 J. D. Hoffman, G. Davis and J. I. Lauritzen, 'In treatise on Solid State Chemistry'; Ed., N. B. Hannay, Plenum Press, New York 1976, Vol 3, Chapter 7.